ELSEVIER

Polymer 42 (2001) 4473–4482

polymer

www.elsevier.nl/locate/polymer

Organic–inorganic networks in foams from high internal phase emulsion polymerizations

H. Tai, A. Sergienko, M.S. Silverstein*

Department of Materials Engineering, Technion — Israel Institute of Technology, Haifa 32000, Israel

Received 27 September 2000; received in revised form 1 November 2000; accepted 8 November 2000

Abstract

Hybrid foams, which combine an inorganic polysilsesquioxane network with an organic polystyrene network, were successfully synthesized using high internal phase emulsions (HIPE). Methacryloxypropyltrimethoxysilane (MPS) was copolymerized radically with styrene (S) and divinylbenzene (DVB) in the organic phase of the emulsion. The hydrolytic condensation of the trimethoxysilyl groups formed an inorganic polysilsesquioxane network, which significantly increased the high temperature modulus and thermal stability of the foam. The hybrid foam had an open-cell structure typical of polymer foams based on HIPE (polyHIPE), with a significantly smaller cell diameter than S/DVB polyHIPEs. In the absence of DVB, there is no crosslinked network to restrict the mobility of MPS and the polysilsesquioxane network is more fully developed. At low MPS contents, the thermal stability of the foams is higher for foams with DVB, reflecting their higher crosslinking density. At high MPS contents, the thermal stability is higher for foams without DVB, reflecting the more fully developed inorganic network.

Keywords: Hybrid foam; High internal phase emulsion (HIPE); Polysilsesquioxane

1. Introduction

High internal phase emulsions (HIPEs) are emulsions in which the dispersed phase occupies more than 74% of the emulsion volume, i.e. more than the maximum packing fraction for identical spheres [1,2]. HIPE can be used as templates for the production of highly porous (cellular) polymeric materials, known as polyHIPE [3]. The cellular structure of a polyHIPE is isotropic and quite different from the oriented structure of commercial blown and extruded foams. Several high temperature HIPE foams have been investigated: the copolymerization of N-substituted maleimide and bismaleimide [4–6] and the copolymerization of a maleimide-terminated aryl ether sulfone macromonomer using a nonaqueous HIPE [7]. Polymers with polar groups usually have high thermal stabilities. The monomers involved, however, are often water-soluble and thus not suitable for HIPE formation.

Polysilsesquioxanes have attracted much attention for their extraordinary heat and fire resistance [8]. They are most broadly described by an empirical formula $(RSiO_{1.5})_n$, where R is an alkyl group, hydrogen, or a combination of different alkyl groups. They can be prepared from the hydrolytic condensation of organotrialkoxysilanes [9], $RSi(OR')_3$ or $RSiX_3$, where R' is an organic group and X is a halogen.

In this paper, we describe the simultaneous synthesis within a HIPE of an organic polymer network and an inorganic polysilsesquioxane network. This foam was prepared from methacryloxypropyltrimethoxysilane (MPS, a vinylsilane), and styrene. The MPS/styrene copolymerization proceeds via the vinyl group using a typical radical mechanism [10] with a water-soluble initiator. The monomers in the MPS/S copolymerization [11] have similar reactivity ratios ($r_1 = 0.58$, $r_2 = 0.36$) and, therefore, a uniform copolymer was expected. The combination of vinyl radical polymerization with trimethoxysilane hydrolysis and condensation in a HIPE was expected to yield an organic–inorganic hybrid foam, possessing unique properties, including higher thermal stability. The three reactions involved in the formation of the organic–inorganic hybrid foam are illustrated in Fig. 1. For illustrative purposes, the radical copolymerization is shown proceeding prior to hydrolysis, although this is not necessarily the case.

* Corresponding author. Tel.: +972-4-829-4582; fax: +972-4-832-1978.
E-mail address: michaels@tx.technion.ac.il (M.S. Silverstein).

0032-3861/01/$ - see front matter
PII: S0032-3861(00)00820-X

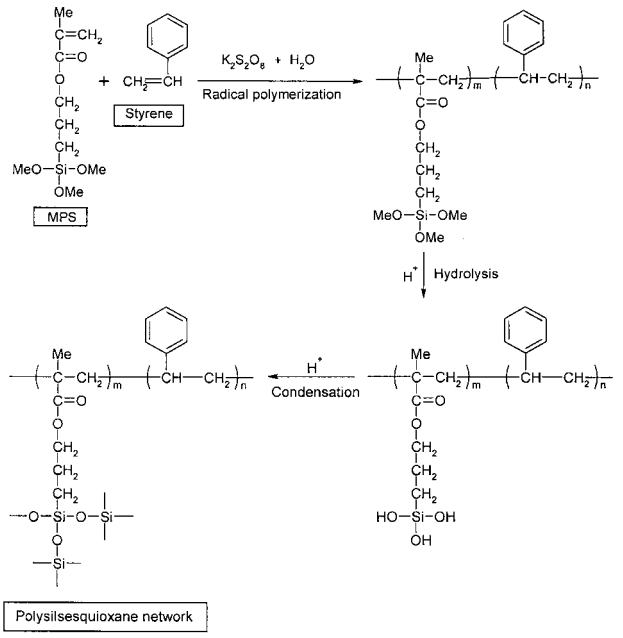

Fig. 1. Schematic illustration of the reactions involved in the formation of hybrid foams.

2. Experimental

2.1. Materials

The monomers used were styrene (purity >99%, Fluka Chemie), MPS (Fluka company, 98% content), and commercial divinylbenzene (DVB) which is 80% DVB and 20% ethyl styrene (Fluka). All monomers were used without removing their inhibitors. The initiator was potassium peroxodisulfate ($K_2S_2O_8$, purity >99%, Riedel-de Haen). The emulsifier was sorbitan monooleate (SMO, Span 80, Sigma-Aldrich Chemie Co.). Calcium chloride hydrate ($CaCl_2{\cdot}2H_2O$, Chemical pure, ACS Co.) was used as an electrolyte to stabilize the HIPE. Cyclohexane (purity >99%, Acros Organics) was used to stabilize the 100% MPS foam.

Table 1
Foam compositions

Foam	MPS (ml)	Styrene (ml)	DVB (ml)	Span 80 (g)
CTS00	0	9	1	2
CTS20	2	7	1	3
CTS40	4	5	1	3
CTS60	6	3	1	3
CTS80	8	1	1	4
TS10	1	9	0	3
TS30	3	7	0	3
TS50	5	5	0	3
TS70	7	3	0	3
TS100[a]	10	0	0	4.5

[a] 5 ml cyclohexane was added to the organic phase to yield a stable HIPE.

2.2. Foam preparation

The foam compositions are listed in Table 1. The oil phase consists of the monomers and emulsifier. The aqueous phase consists of deionized water, initiator and salt. The oil phase was mechanically stirred in a 250 ml beaker while 100 g of deionized water containing 0.2% potassium persulfate and 0.5% $CaCl_2{\cdot}H_2O$ was added slowly. After all the aqueous phase had been added, the HIPE was stirred for an additional 5 min. An additional 20 ml of aqueous phase was added to the HIPE surface and formed a layer above the HIPE surface that prevented monomer evaporation and kept the surface wet. The pH of the aqueous phase was measured several times during the synthesis. The beaker was sealed using Saran Wrap and put in a convection oven at 65°C for 24 h for polymerization and crosslinking. The viscosity of the HIPE increased with MPS content, reflecting its effect on the interfacial tension and, possibly, the effects of the increasingly prevalent hydrolysis and condensation. A HIPE could not be formed using MPS as the only monomer. Adding 5 ml cyclohexane to the oil phase yielded a stable HIPE, which was used to synthesize a polyHIPE foam, TS100. TS100, however, was so brittle that it shattered during drying.

After polymerization, the foams were removed from the beaker, put into a convection oven and dried to constant weight at 80°C. The drying time varied from several to 48 h. Foam TS70 was not completely dry after 48 h at 80°C and was therefore dried for an additional 24 h at 120°C. The first set of hybrid polyHIPE, those that contained 10% DVB, were postcured in a vacuum oven at 250°C overnight, in an attempt to remove the emulsifier. This postcuring did not seem to have a significant effect on the polyHIPE. The second set of hybrid polyHIPE foams, those without DVB, were not postcured.

The inner diameter of the synthesis beaker (d_0) was measured. The sample diameter was measured both before (d_p) and after (d_d) drying. The linear shrinkage during polymerization (S_p, %), Eq. (1), and the linear shrinkage during drying (S_d, %), Eq. (2) were calculated based on the change in diameter.

$$S_p = (d_0 - d_p)/d_0 \times 100\% \quad (1)$$

$$S_d = (d_0 - d_d)/d_0 \times 100\% - S_p \quad (2)$$

The measured weight loss (W_a) is the difference between the total weight of all the components except the deionized water and the weight of the dried foam.

2.3. Characterization

The foam density was determined from weight and volume measurements. The structure was characterized using high-resolution scanning microscopy (HRSEM; LEO 982, Zeiss Company, Germany) of cryogenic fracture

Table 2
Foam behavior and properties

Foam	Weight loss (g)			Shrinkage (%)		Density (g/cm)^3	T_g (°C)
	W_a	W_b	W_c	S_p	S_d		
CTS00	1.68	0	0	1.1	6.2	0.11	148
CTS20	2.42	0.74	0.56	1.6	1.3	0.09	158
CTS40	3.01	1.33	1.12	3.0	1.4	0.10	161
CTS60	3.65	1.97	1.68	5.1	0.6	0.11	–
CTS80	4.23	2.55	2.24	7.5	0.5	0.12	–
TS10	2.02	0.34	0.28	8.4	19.6	0.19	115
TS30	2.74	1.06	0.84	4.8	2.6	0.13	132
TS50	3.11	1.43	1.40	5.1	0.5	0.10	134
TS70	3.63	1.95	1.98	7.0	0.1	0.11	142

surfaces. No coating was used with the accelerating voltage of 1 kV.

The thermal and mechanical properties were characterized using compressive dynamic mechanical thermal analysis (DMTA) temperature sweeps at 1 Hz and 3°C/min. Compressive stress–strain experiments were also performed using the Rheometrics DMTA. The foam modulus (E_f) was obtained by linear regression of the linear compression region at small strains in the stress–strain curves. The polymer modulus (E_p) has been related to the foam modulus, foam density (ρ_f) and polymer density (ρ_p) as seen in Eq. (3). E_f and ρ_f are measured experimentally, while ρ_p is expected to be in the neighborhood of 1 g/cm^3 for the various polymers. The polymer compressive modulus was calculated using Eq. (1), assuming $\rho_p = 1$ g/cm^3.

$$E_p = E_f\left(\frac{\rho_p}{\rho_f}\right)^2 \tag{3}$$

The thermal stability was characterized using thermogravimetric analysis, TGA, and differential thermal analysis, DTA (TGA–DTA simultaneous analyzer, SDT2960, a module of TA INST 2000, TA-Instruments Company). Foams without DVB were run at 20°C/min from 30 to 650°C in a nitrogen environment (50 cm^3/min). Foams with DVB were run at the same rate from 100 to 800°C in both static air and N_2 environments. The decomposition temperature (T_d) of the foam was defined as the peak position found from the derivative of mass loss with temperature (DTG). The decomposition rate was highest at T_d.

3. Results and discussion

3.1. Synthesis

The pH was 7 at the beginning of the polymerization, 3–4 after 3 h of polymerization and 1–2 by the end of the polymerization (24 h). The changes in pH were the same for the various compositions. The increase in acidity results from the decomposition of the potassium peroxodisulfate initiator during the polymerization. The increasing acidity of the aqueous phase, which is in intimate contact with the organic phase, is expected to function as a catalyst and accelerate the hydrolysis and condensation of the trimethoxysilyl groups.

The weight loss, shrinkage and density of the hybrid foams are listed in Table 2. The measured weight loss (W_a) is calculated by subtracting the weight of the dried foam from the total weight of the HIPE excluding water (i.e. monomers, Span 80, $CaCl_2$, $K_2S_2O_8$). The theoretical weight loss (W_c) is calculated assuming a full hydrolytic condensation of MPS, i.e. the weight loss of 27.8% when MPS changes from R–Si(OCH$_3$)$_3$ to R–SiO$_{1.5}$. The weight loss for the PS foam (W_a^{CTS00}) was 1.68 g. This weight loss is attributed to mass loss from the emulsifier, stabilizer, initiator, and residual monomer removed on drying as well as a small amount of HIPE that may have adhered to the stirrer and the beaker wall. This 1.68 g mass loss is assumed to be constant for all the foams. The weight loss beyond 1.68 g, W_b, is attributed to the hydrolysis and condensation of –Si(OCH$_3$)$_3$ (Eq. (4)).

$$W_b = W_a - W_a^{CTS00} \tag{4}$$

W_b increases with MPS content (Table 2), reflecting the increase in the hydrolysis and condensation of trimethoxysilane. W_b, calculated from the experimental results, is quite close to W_c (Table 2), derived theoretically. Thus, the increase in W_a with increasing MPS content reflects close to complete hydrolysis and condensation of trimethoxysilane.

For the foams with DVB, the shrinkage during polymerization increased markedly with increasing MPS concentration. The shrinkage during polymerization reflects the bulk contraction resulting from both radical vinyl polymerization and the hydrolysis and condensation of –Si(OCH$_3$)$_3$. There is a relatively small shrinkage of 1.1% for CTS00 during polymerization. The increase in hydrolysis and condensation with increasing MPS content yields an increase in the shrinkage during polymerization (Table 2) which reflects

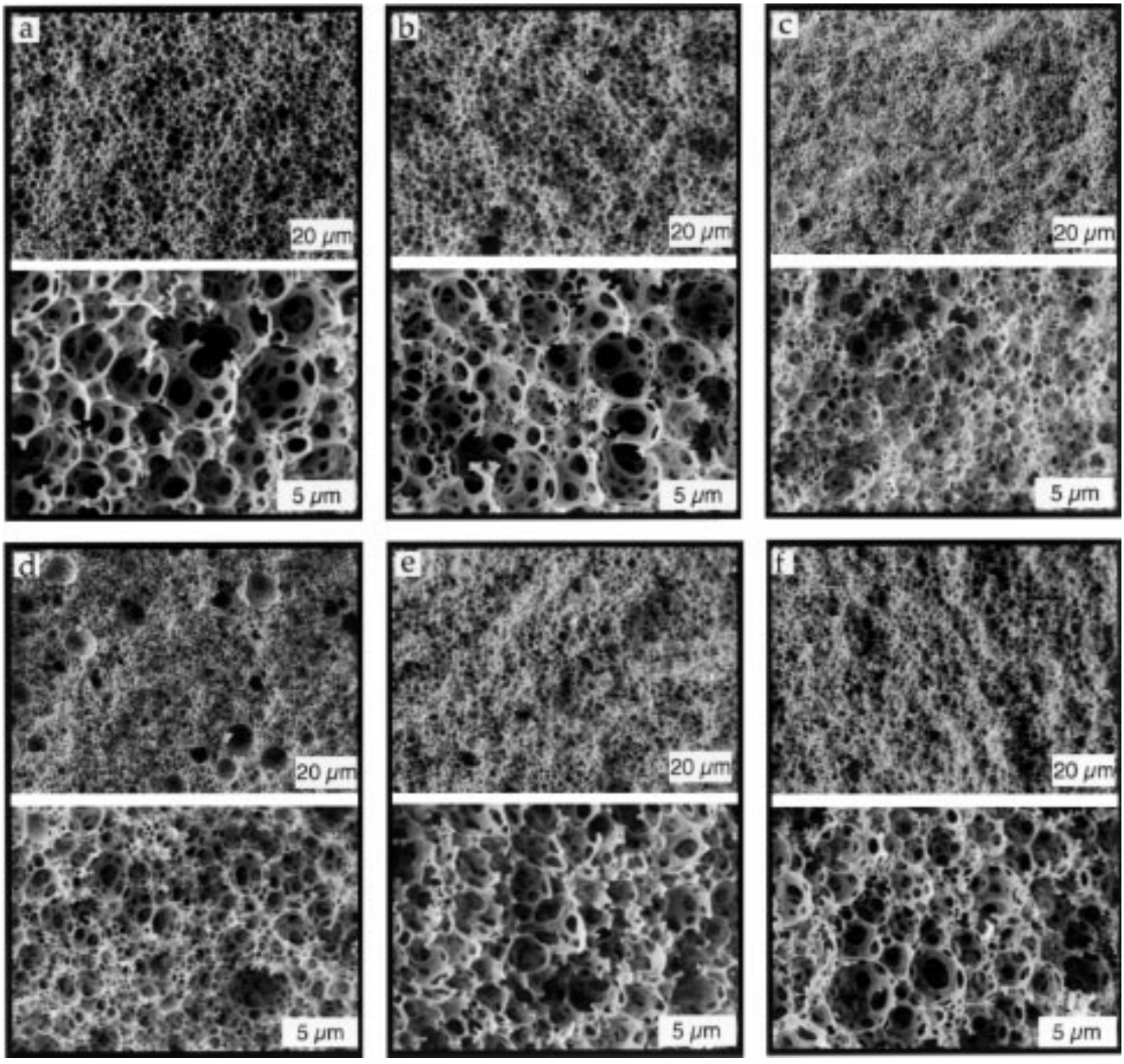

Fig. 2. HRSEM micrographs of foam cryogenic fracture surfaces at two magnifications: (a) CTS00; (b) CTS20; (c) CTS40; (d) CTS60; (e) TS10; (f) TS30.

the increase in mass loss. The shrinkage during drying, on the other hand, decreases with increasing MPS concentration. The addition of MPS increases crosslinking density and chain stiffness, enhancing the ability of the foam to maintain its shape during drying.

Hybrid foams without DVB exhibit behavior similar to that of foams with DVB. The increase in mass loss, increase in shrinkage during polymerization and decrease in shrinkage during drying corresponds to the increase in MPS content. TS10 exhibits exceptionally high shrinkage both during polymerization and drying. The high shrinkage reflects the particularly low crosslinking density in TS10, which includes no DVB and only 10% MPS.

The density of the hybrid foam reflects both the weight loss and shrinkage. CTS20 combines low weight loss (little MPS) with low shrinkage (enough MPS to enhance stiffness and crosslinking) to yield a density of 0.09 g/cm^3. The relatively high shrinkage in TS10 yields the relatively high density of 0.19 g/cm^3.

3.2. Morphology

The morphology of the P(S/DVB) foam (CTS00) in Fig. 2a is typical of polyHIPE. The cells, approximately 4 μm in diameter, have a narrow size distribution (Fig. 2a, upper), as do the intercellular pores in the cell walls (Fig. 2a, lower). The intercellular pores, about 1 μm in diameter, yield the highly open-cell structure.

All the hybrid foams with DVB (Fig. 2b–d) exhibit the typical polyHIPE foam structure seen for P(S/DVB). The

average cell diameter decreased dramatically with the addition of MPS. CTS20 had an average cell diameter of about 4 μm (Fig. 2b, lower), similar to that of the P(S/DVB) foam. The average cell diameters for CTS40 (Fig. 2c, lower), CTS60 (Fig. 2d, lower) and CTS80 (not shown) lie between 1 and 2 μm, less than half that of the P(S/DVB) foam. The decrease in the average cell size may reflect a reduction in interfacial tension on incorporation of the more hydrophilic MPS. At higher MPS contents, a number of large cells are observed such as those in CTS60 (Fig. 2d, upper). Almost no large cells are observed for CTS20 (Fig. 2b, upper) and CTS40 (Fig. 2c, upper). The large cells are formed when there is a significant increase in HIPE viscosity, which occurs when high water-to-oil ratios are reached for high MPS contents. The high viscosity may reflect not only the different hydrophilicities of MPS and styrene, but may also reflect some initial hydrolysis and condensation and the beginning of inorganic network formation. At high viscosities, the shear stress of mixing is not able to break up the large droplets. It is thus difficult to generate a uniform, fine dispersion of the aqueous phase in those HIPE which are highly viscous at high water/oil ratios [12].

Cameron [13] has reported that adding 4-vinylbenzyl chloride (VBC) can reduce the cell size of polyHIPE foams. He ascribed this phenomenon to the adsorption of VBC at the interface and the subsequent reduction in interfacial tension. MPS may also act as a co-surfactant and be preferentially absorbed at the interface. On one hand, the increase in MPS content reduces interfacial tension, and thus reduces cell dimensions. On the other hand, the increase in MPS content increases the viscosity at high water-to-oil ratios and makes it more difficult to generate the mixing shear stress needed to create a fine dispersion of the aqueous phase, yielding large droplets in the last stage of HIPE synthesis. Viscosity thus plays an important role in determining cell size and size distribution.

When the MPS content is less than 70%, the hybrid foams without DVB exhibit the typical polyHIPE cellular structure. This indicates that crosslinking through silanol condensation occurs and prevents the collapse of the cellular structure. In spite of the 28% shrinkage on drying, and the relatively high density, TS10 (Fig. 2e) has cells of about 2.5 μm in diameter. The average cell diameter for TS30 (Fig. 2f) is about 3 μm and that for TS50 (not shown) is under 2 μm.

A longer time and a higher temperature were needed to dry TS70 than were needed to dry the other foams. This indicates that TS70 did not have the highly open-cell structure typical of the polyHIPE. The morphology of TS70 (Fig. 3a) is quite different from that of the other foams. There are exceptionally large cells, macro-cells, 80–150 μm in diameter, separated by thick, porous walls. The structure within the walls is reminiscent of the typical polyHIPE cellular structure, with cells of about 1.5 μm in diameter (Fig. 3b). These thick walls are the remnants of the original polyHIPE structure. The macro-cells in Fig. 3a are filled with particles of about 1 μm in diameter that form clumps (Fig. 3c). The collapse of the original HIPE structure, into thick walls surrounding macro-cells, yields an inhomogeneous structure. This collapse occurs without affecting the external dimensions of the foams and its density.

The change in interfacial tension on addition of MPS, which yields the smaller cells, may also increase intercellular pore density and reduce wall thickness. The thinner,

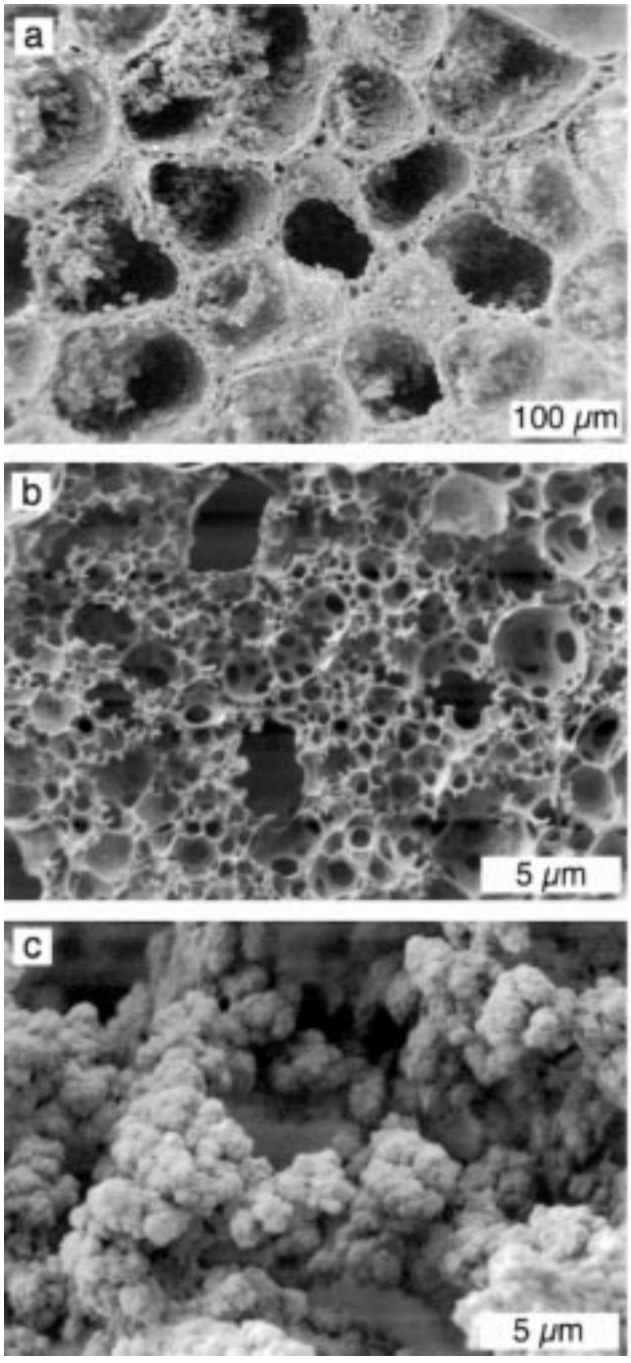

Fig. 3. HRSEM micrographs of foam TS70 cryogenic fracture surface: (a) low magnification of both macro-cells and thick walls; (b) high magnification of the thick walls; (c) high magnification of the macro-cells.

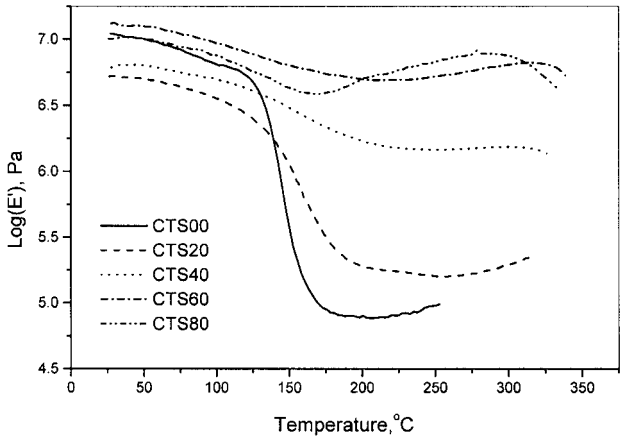

Fig. 4. Variation of E' with temperature for the foams with DVB.

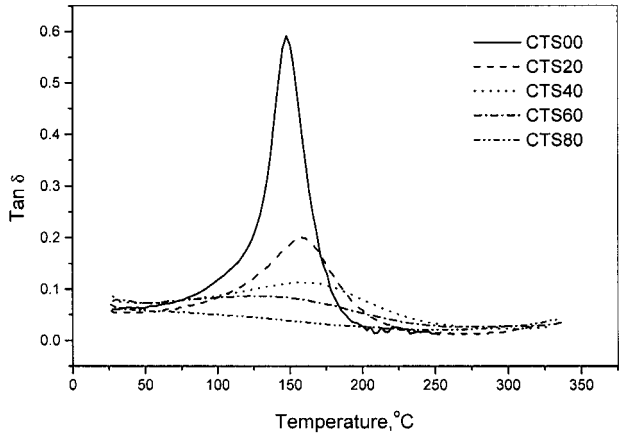

Fig. 5. Variation of tan δ with temperature for the foams with DVB.

more porous walls with a higher degree of curvature that could result from a reduction in interfacial tension would be more prone to collapse and coalescence. The stability introduced by the formation of a DVB crosslinked network prevents this catastrophic collapse, even at high MPS contents, i.e. CTS80.

3.3. Thermal mechanical properties

The variation of E' with temperature for the hybrid foams with DVB is seen in Fig. 4. The slight variations in the moduli at low temperature reflect the variations in foam density. CT20 has the lowest density (0.09 g/cm^3) and therefore the lowest modulus; CTS80 has the highest density (0.12 g/cm^3) and therefore the highest modulus. The moduli of the glassy polymers in the foams are expected to be quite similar at low temperatures. The decrease in modulus at about 130°C, seen for the foams with low MPS contents, reflects the glass transition. At temperatures above the glass transition, the modulus increases with MPS content by about two orders of magnitude, from the foam without MPS (CTS00) to the foam with 80% MPS (CTS80). Above the T_g, the organic network is soft and rubbery, while the polysilsesquioxane inorganic network is stiff and rigid. A small reduction in sample thickness and the corresponding increase in density at high temperatures yield the slight increase in apparent modulus. The modulus of the hybrid foams remains high until the beginning of degradation.

The variation of tan δ with temperature for the foams with DVB is seen in Fig. 5. The tan δ peak becomes increasingly broader and smaller with MPS content. The T_gs, taken from the tan δ peaks, are listed in Table 2. At low MPS concentrations, the T_g increases with MPS content, up to 161°C for 40% MPS. The tan δ peak for CTS60 is so broad that a T_g cannot be accurately assigned. At 80% MPS, the styrene becomes a minor component and no tan δ peak could be discerned. The increase in crosslinking density increases the T_g, broadens the tan δ peak and produces a significant reduction in its height.

The incorporation of MPS also enhances the dimensional stability. During the DMTA measurement, there was a significant decrease in the CTS00 cross-section. The changes in the dimensions of the hybrid foams (CTS20 to CTS80) were relatively negligible up to 300°C. The inorganic silsesquioxane network thus yields a thermally and dimensionally stable material with a relatively high modulus at temperatures above the T_g associated with PS.

The variation of storage modulus with temperature for hybrid foams with no DVB (not shown) is similar to that of the hybrid foams with DVB. As seen for the foams with DVB, the modulus at temperatures above the T_g associated with P(S/DVB) increases significantly with MPS content and the modulus remains relatively unchanged until about 300°C. The modulus above the T_g associated with PS increases by approximately two orders of magnitude from TS10 to TS70, reflecting the increasing predominance of the silsesquioxane network with the increasing MPS content. The changes in the position and shape of the tan δ peak with MPS content for foams with and without DVB (not shown) are similar. The T_gs from the tan δ peaks are listed in Table 2. The T_g increases with MPS content, reflecting the increase in crosslinking density. The absence of DVB and the organic network is reflected in the lower T_gs for similar styrene contents.

3.4. Mechanical properties

The compressive strain–stress curves at 30 and 250°C for CTS00 and CTS80 are seen in Fig. 6. The compressive strain–stress curves for CTS00, as well as for CTS20 and CTS40 (not shown) at 30°C are typical three-stage foam compressive strain–stress curves: a linear elastic region, a plateau region and a bulk compression region [14]. CTS60 and CTS80 failed at 30°C in a brittle manner. The length of the plateau region and the strain at which the bulk

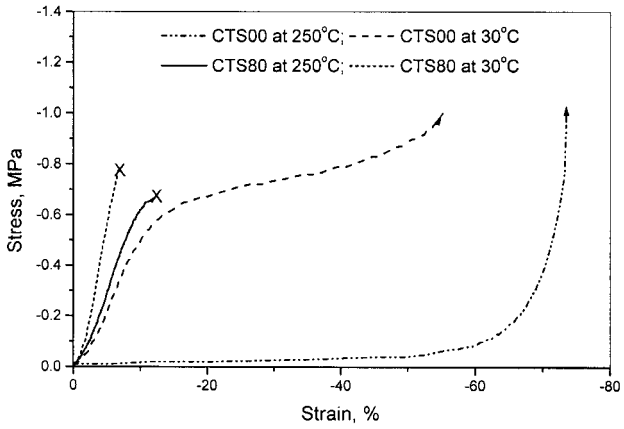

Fig. 6. Compressive stress–strain curves for CTS00 and CTS80 at 30 and 250°C.

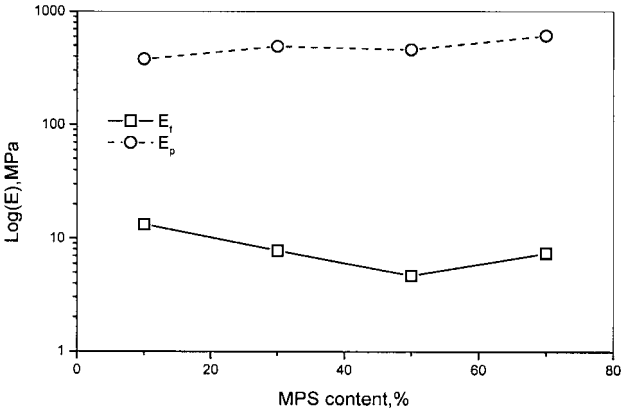

Fig. 8. Variations in the foam and polymer moduli at 30 and 250°C with the MPS content for the foams without DVB.

compression begins both decrease with increasing MPS content. The modulus and strength decreased with temperature, while the strain at break increased.

The foam modulus was calculated from the elastic region of the compressive strain–stress curve. The variations in the polymer and foam moduli with MPS content, both at 30 and at 250°C, are seen in Fig. 7. The foam and polymer moduli behave in a similar fashion, since the densities of the foams are similar. The modulus at 30°C is relatively independent of MPS content, reflecting the relative insensitivity of the glassy polymer to the degree of crosslinking. There is, however, a slight increase in modulus with MPS content. The modulus at 250°C increases substantially with MPS content, reflecting the importance of the polysilsesquioxane network above the T_g associated with PS. The modulus at 250°C approaches that at 30°C with increasing MPS content, as the stiff polysilsequioxane network becomes dominant.

TS10, TS30 and TS50 also exhibited three-stage compressive strain–stress curves (not shown) typical of foams. TS70 failed in a brittle manner, at a relatively low strain, with a compressive strength of 0.5 MPa (not shown). The variations in the foam and polymer moduli at 30°C with the MPS content for the foams without DVB are seen in Fig. 8. The decrease in foam modulus with MPS content between 10 and 50% MPS results from the significant decrease in foam density. The polymer modulus is relatively MPS independent, increasing slightly with crosslinking density, as expected.

3.5. Thermal degradation

TGA curves for the foams with DVB, in both nitrogen and in air are seen in Fig. 9. A one step degradation process is observed and the thermal stability (temperature at which decomposition starts) decreases with increasing MPS concentration. The decomposition temperature (T_d) was determined from the first derivative of the TGA curve. The variations of T_d with MPS content are seen in Fig. 10. For the hybrid foams with DVB (CTS foams), T_d in N_2 decreases substantially with MPS content, from 438°C for

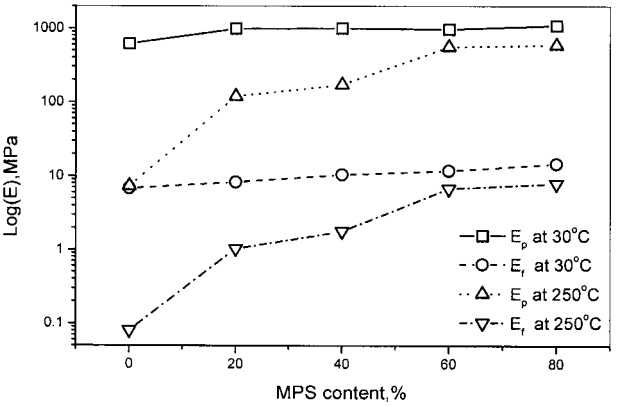

Fig. 7. Variations in the foam and polymer moduli at 30 and 250°C with the MPS content for the foams with DVB.

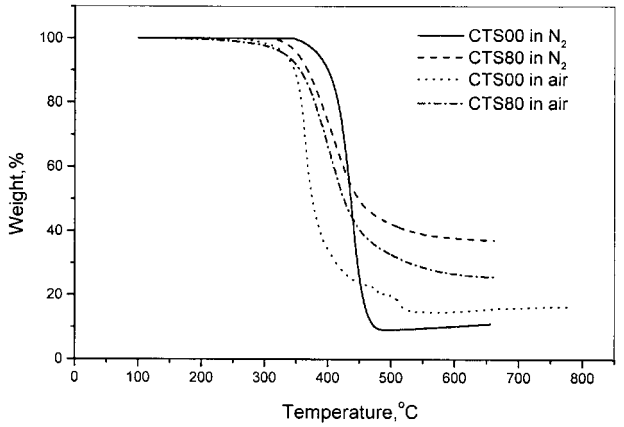

Fig. 9. TGA curves for the foams with DVB.

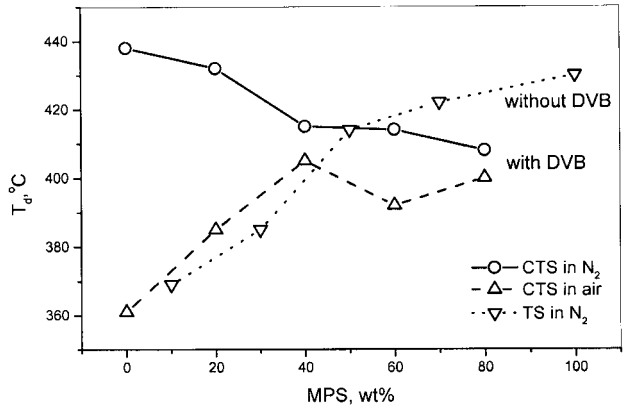

Fig. 10. Variation of T_d, in either N_2 or static air, with the MPS content.

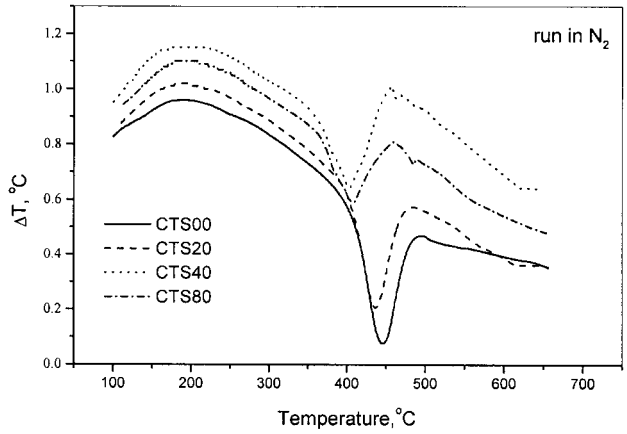

Fig. 12. DTA curves for the foams with DVB run in N_2.

CTS00 to 408°C for CTS80. The degradation ceiling temperatures for PMMA and PS are 220 and 300°C [15], respectively, indicating that PS is significantly more thermally stable than PMMA. Introducing the methacrylate group of MPS into the polymer molecule through copolymerization reduces the thermal stability of the poly-HIPE.

The T_d in air is lower than T_d in N_2 (Fig. 10), since the presence of oxygen reduces the activation energy for degradation [15]. As opposed to the trend seen for the T_d in N_2, the T_d in air increases with MPS content until they almost coincide at high MPS contents. The presence of the inorganic polysilsesquioxane network thus increases the stability of the foams in air. The oxygen reacts with the inorganic network to yield silica, imparting thermal stability. The reaction of oxygen with the inorganic network delays degradation of the organic material and yields the increase in T_d with MPS content. At low MPS contents the T_d in air is significantly below that in N_2, reflecting the predominant oxidation of styrene. At high MPS contents the T_d in air is only slightly less than that in N_2, reflecting the predominant oxidation of the polysilsesquioxane network.

The TGA curves for hybrid foams without DVB (TS foams) in N_2 are similar to those of the hybrid foams with DVB in air. There is a 60°C increase in the TS foam T_d with increasing MPS content (Fig. 10). The T_d is lower for the foams without DVB when the MPS content is less than 50%, reflecting the low degree of crosslinking. The polysilsesquioxane inorganic network is expected be more pervasive and predominant in the absence of DVB. The formation of a DVB network limits the mobility of the silane groups and thus limits their ability to form a pervasive network. The T_d is higher for the foams without DVB when the MPS content is greater than 50%, reflecting the predominance of the polysilsesquioxane network.

The variation of the TGA residual mass at 500°C with MPS content is seen in Fig. 11. The residual mass from the foams with DVB (CTS) increases substantially with MPS content, both in N_2 and in air. For the hybrid foams without DVB (TS), the residual mass also increases with MPS

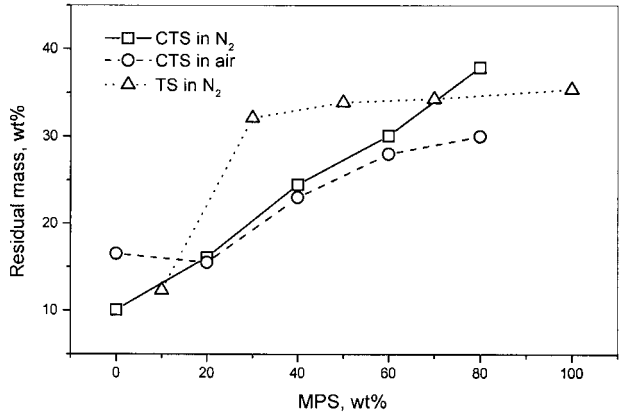

Fig. 11. Variation of the TGA residual mass at 500°C with the MPS content.

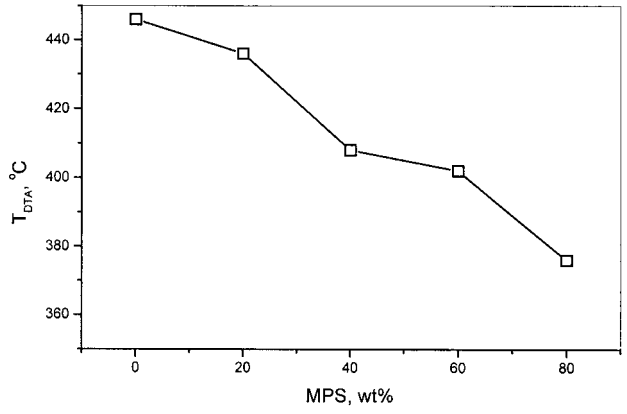

Fig. 13. Variation of DTA peak temperature with composition for foams with DVB.

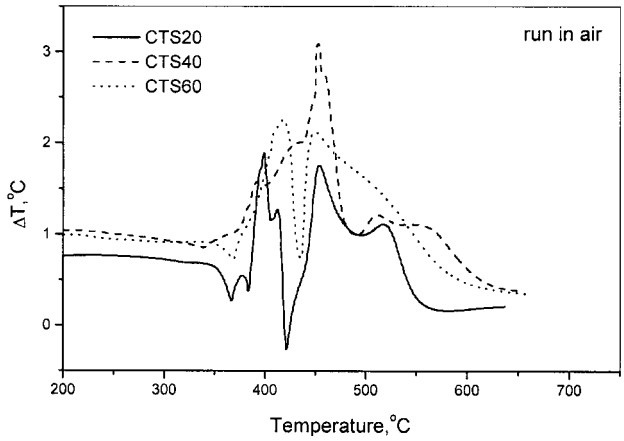

Fig. 14. DTA curves for the foams with DVB run in air.

content. The 32% residual mass for TS30 is significantly higher than the 10% for TS10 and the residual mass that could be expected for a 30% MPS foams with DVB from the results in Fig. 11. This high residual mass for TS30 reflects the formation of a dense silsesquioxane network, which entraps the organic material when the silane mobility is not limited by DVB crosslinking. There is only a slight increase in the residual mass with further increases in MPS content for the foams without DVB.

DTA curves for the foams with DVB run in nitrogen are seen in Fig. 12. The endothermal DTA peak that corresponds to decomposition becomes smaller and occurs at lower temperatures with increasing MPS concentration. The variation of the DTA peak temperatures with MPS content for runs in N_2 is seen in Fig. 13. The decrease in DTA peak temperature with MPS content reflects the reduction in thermal stability introduced by copolymerization with a methacrylate. The decrease in peak area with MPS content reflects the increase in the polysilsesquioxane content.

The DTA curves for the foam with DVB run in air are seen in Fig. 14. The differences in the degradation mechanisms in air and in N_2 can be seen from the DTA curves. There are both endothermal peaks and exothermal peaks for the DTA in air. The endothermal peaks represent thermal decomposition while the exothermal peaks represent thermal oxidation. The exothermal oxidation peak becomes predominant and shifts to higher temperatures with increasing MPS content. This exothermal peak represents the oxidation of the silsesquioxane network to SiO_2.

4. Conclusions

Organic–inorganic hybrid open-cell foams were prepared successfully by copolymerizing MPS and styrene in HIPEs. Both the mechanical properties at high temperatures and the thermal stability of the foams were improved dramatically on the formation of polysilsesquioxane inorganic networks through the copolymerization of styrene and MPS. The mechanical properties, dimensional stability and thermal stability were further enhanced on the formation of organic–inorganic hybrid networks through the combination of MPS and DVB.

All the hybrid foams except TS70 have typical polyHIPE cell structures. Increasing the concentration of MPS reduces the interfacial tension and produces a marked reduction in cell diameter.

The incorporation of MPS into the polymer and the formation of the polysilsesquioxane network yields an increase in the glass transition associated with PS of up to 20°C and an increase of up to two orders of magnitude in the modulus at temperatures above the T_g.

Foams with over 40% MPS exhibit a high modulus until degradation begins. For the hybrid foams without DVB, the thermal stability of the foam in N_2 increases significantly with MPS content due to the increase in crosslinking density. At low MPS concentrations, the thermal stability in N_2 of the hybrid foams with DVB was greater than that of the foams without DVB. The higher stability reflects the significantly higher crosslinking density in the foams with DVB. The decrease in thermal stability in N_2 with MPS content for the foams with DVB reflects the lower stability of the polymethacrylate segments from MPS. The increase in thermal stability in air with MPS content for the foams with DVB reflects the increasingly predominant oxidation of the silsesquioxane network to SiO_2.

Acknowledgements

We acknowledge the assistance of Miss Ji Rongqin of Hebei University of Technology, China for TGA–DTA measurements and the partial support of the Technion VPR Fund and the Goldsmith Visiting Scientist Fund.

References

[1] Lissant KJ. Emulsions and emulsion technology, Part 1. New York: Marcel Dekker, 1974 (chap. 1).
[2] Cameron NR, Sherrington DC. Adv Polym Sci 1996;126:163–214.
[3] Barby D, Haq Z. US Pat 4,522,953, 1985.
[4] Hoisington MA, Duke Jr. JR, Apen PG. Polymer 1997;38(13):3347–57.
[5] Duke Jr. JR, Hoisington MA, Langlois DA, Benicewicz BC. Polymer 1998;39(18):4369–78.
[6] Hoisington MA, Duke Jr. JR, Langlois DA. Microporous Macroporous Mater 1996;431:539–44 (Mater Res Soc Symp Proc).
[7] Cameron NR, Sherrington DC. Macromolecules 1997;30(19):5860–9.
[8] Zhu B, Katsoulis DE, Keryk JR, McGarry FJ. Polymer 2000;41(20):7559–73.
[9] Loy DA, Schneider DA, Baugher BM, Rahimian K. Book of abstracts, 219th ACS National Meeting, San Francisco, CA, March, 26–30, 2000.
[10] Otsu T, Endo K, Tanaka M. Mem Fac Engng 1988;29:151–9.

[11] Spychal S, Krolikowski W. Polymer 1984;29(9):343–6.
[12] Tai H, Sergienko A, Silverstein MS. Polym Eng Sci. Accepted for publication.
[13] Barbetta A, Cameron NR, Cooper SJ. Chem Commun 2000:221.
[14] Klempner D, Frisch KC. Handbook of polymeric foams and foam technology. New York: Oxford University Press, 1996.
[15] Chartoff RP. In: Turi EA, editor. Thermal characterization of polymeric materials, New York: Academic Press, 1997.